Surface-Induced Asymmetries during Spinodal Decomposition in Off-Critical Polymer Mixtures†

Georg Krausch* and Edward J. Kramer

Department of Materials Science and Engineering and the Materials Science Center, Cornell University, Ithaca, New York 14853-1501

Frank S. Bates

Department of Chemical Engineering and Materials Science, University of Minnesota, Minneapolis, Minnesota 55455

J. F. Marko

Laboratory of Atomic and Solid State Physics and the Materials Science Center, Cornell University, Ithaca, New York 14853-2501

G. Brown and A. Chakrabarti

Department of Physics, Kansas State University, Manhattan, Kansas 66506

Received January 14, 1994®

ABSTRACT: We have studied the growth of the wetting layer formed at the surfaces of symmetric and nonsymmetric mixtures of poly(ethylenepropylene) (PEP) and perdeuterated poly(ethylenepropylene) (dPEP) during spinodal decomposition. For off-critical quenches, the growth rate is found to be strongly dependent on the bulk composition of the mixtures. If the minority phase wets the surface, the wetting layer is found to grow slower than in the reverse situation, where the majority phase wets the surface. In the latter case, hydrodynamic effects may play a role, increasing the rate of wetting layer growth. The surface spinodal waves are shallower for the case of off-critical compositions as compared to critical compositions. However, independent of bulk composition, all surface composition profiles exhibit universal scaling behavior in the near-surface region. Our conclusions are strengthened by numerical simulations of a diffusively coarsening mixture near a surface that attracts one of the phases. No appreciable acceleration of growth of the surface layer is observed in simulations where the wetting phase is the majority phase, suggesting that the acceleration observed experimentally is due to fluid flow. The simulations also show that there can be "surface-induced nucleation" in the case that the majority phase is attracted by the substrate: the expulsion of minority phase can lower the nucleation barrier near the substrate, causing more droplets to nucleate there than in the bulk.

I. Introduction

Phase separation phenomena have been extensively studied in the past two decades both theoretically and experimentally. While the essential features of phase separation in the bulk are understood, it only recently became clear that, in the vicinity of the surfaces confining any real bulk sample, both the equilibrium phase morphology and the phase separation dynamics may be severely altered. Following the theoretical prediction of Ball and Essery,[1] the first experimental observation of a "surface-directed spinodal decomposition" was reported by Jones and co-workers;[2] thereafter, the effect was studied in a variety of different experiments,[3-7] and phenomenological as well as numerical studies[8-11] were reported. However, this phenomenon is still largely unexplored, due to the diversity of the experimental systems studied thus far and also due to the rich variety of effects reflected in the different time scales that have been established in the study of bulk phase separation.

Quite different pieces of information have accumulated concerning the time dependence of the phase separation in the near-surface region. Cumming and co-workers investigated the growth of lateral surface domains during very shallow quenches of a low molecular weight polymer mixture and found a $t^{3/2}$-growth law, considerably faster than the $t^{1/3}$ behavior commonly found for bulk domains during the late stage of spinodal decomposition.[4] Brown and Chakrabarti performed numerical simulations for rather deep critical quenches, finding the surface domains to grow as $t^{1/3}$ both laterally and perpendicular to the surface;[8] the latter prediction was recently verified for a high molecular weight critical polymer mixture.[7] Tanaka studied phase separation of a polymer/water mixture confined in one- and two-dimensional capillaries for both critical and off-critical quenches;[5] due to the low viscosity this study was concerned with the very late stage of phase separation where hydrodynamic flow governs the material transport between the different domains. While these results are important for understanding the equilibrium phase morphologies found during late-stage phase separation in confined geometries, they are insensitive to the development in the earlier stages of spinodal decomposition and therefore cannot be compared to the investigations performed on polymer melts.[2,3,5-7]

In view of this incomplete picture, we have continued our investigations of surface-directed spinodal decomposition of an isotopic polymer mixture.[2,6,7] The use of well-characterized, isotopic mixtures has proven advantageous for the study of the thermodynamic properties of partially miscible polymer blends; they are "ideal" systems that can be closely compared to theoretical predictions because the mechanical and rheological properties of the two species are almost identical and the demixing interaction is due solely to van der Waals interactions. In a recent study,[7] we showed that for critical compositions the wetting

† Report No. 7624 issued by the Materials Science Center.

* To whom correspondence should be addressed. Present address: Fakultät für Physik, Universität Konstanz, Postfach 5560, D-78434 Konstanz, Germany.

® Abstract published in *Advance ACS Abstracts*, October 1, 1994.

0024-9297/94/2227-6768$04.50/0

layer which forms during spinodal decomposition thickens with time t as $t^{1/3}$, in agreement with theoretical predictions for the diffusive stage of the phase separation process. Moreover, it was found that the composition profiles perpendicular to the surface exhibited universal scaling behavior; i.e., they collapse onto a single, time-independent master curve when distance is rescaled by the wetting layer thickness.

In section II, we describe the extension of our experiments to a broader time range as well as to off-critical compositions. In contrast to the situation in bulk, in the near-surface region, strong asymmetries in the growth behavior should be observable, since the attractive interaction between the surface and one of the two components breaks the symmetry between the two complementary compositions Φ and $1 - \Phi$ in a system with a symmetric phase diagram. Depending on whether the minority phase is, or is not, the wetting phase attracted to the film surface, differences in the surface domain growth should occur. These asymmetries are indeed observed. In addition, we show that the scaling behavior of the composition profiles holds, independent of the bulk composition.

In section III, we describe numerical studies of the behavior of the Cahn–Hilliard–Cook (CHC) equation[12] in the vicinity of a surface in two and three dimensions in order to determine whether the good agreement with experiment that was previously found for critical concentrations[6] could be extended to off-critical concentrations. (In this paper CHC refers to the Cahn–Hilliard theory, plus thermal noise and nonlinearities—this is variously called the nonlinear Cahn–Hilliard–Cook model, or Model B, or the conserved-order-parameter time-dependent Ginzberg–Landau equation.[12]) Diffusion is the only transport process included in the CHC model. Our simulations indicate that the surface domains in this model thicken as $t^{1/3}$, even for off-critical quenches. There is a slight change in the prefactor of this growth law with concentration, but the simulations do not show the rapid increase in thickness of the surface layer that we observe experimentally when the majority phase wets the surface. Thus our simulations do not show the strong growth-law asymmetry observed experimentally. We take this as evidence that the experimental effect is due to physics not included in the CHC equation—the most obvious alternate transport mechanism is hydrodynamic flow driven by interfacial tension.[13]

In section IV, we discuss the various regimes revealed by these studies. We review the scaling theory for Lifshitz–Slyozov[14] coarsening ($t^{1/3}$ or diffusive coarsening) applied to surface layer growth, which describes most of the experiments. We will then show that the growth law proposed by Siggia[13] for bulk domains, and later argued by one of us[10] to describe surface layer thickening in liquid mixtures, describes the fast thickening of a majority wetting phase.

II. Experiments on Polymer Mixtures

(a) Procedure. The system under experimental study is an isotopic mixture of poly(ethylenepropylene) (PEP) and its deuterated analog (dPEP), both of about equal degree of polymerization ($N_{PEP} = N_{dPEP} = 2286$). The polymers were synthesized following standard procedures.[15] Slight differences in bond length and polarizability between the C–H and the C–D bonds lead to a small unfavorable interaction between the two isotopic species, characterized by a small positive interaction parameter χ.[16,17] For sufficiently long chains, this in turn results in a miscibility gap in the phase diagram; for the molecular weights used in the present study, a critical temperature of 365 K is found. The deuteration as well leads to a small difference in surface energy between the two isotopic species; the deuterated component therefore tends to segregate to the polymer–vacuum interface.[18]

Thin PEP/dPEP films of varying bulk composition were spun cast from toluene solution onto Si substrates. The film thickness was kept well above 2000 nm. The films were annealed in vacuum for different times ranging from 10 min up to as long as several weeks. Annealing temperatures of 294 and 321 K were chosen; these correspond to reduced quench depths of $0.81T_c$ and $0.85T_c$, respectively. Since the glass transition temperature of PEP is well below room temperature, the samples were investigated immediately after annealing if possible; if necessary, the samples were stored under liquid N_2 to prevent any uncontrolled phase separation from occurring at room temperature.

Composition versus depth profiles of the two components were established using time-of-flight foward recoil spectrometry (TOF-FRES). This technique is based on conventional forward recoil spectrometry, where H and D nuclei are elastically scattered from an incident He beam (E_0 = 2 MeV) impinging on the sample under a small angle. The energy of the scattered particles is measured and countrate vs energy spectra are stored; these spectra are then readily converted into concentration vs depth profiles for the two hydrogen isotopes by use of tabulated values for the specific energy loss of the particles on their paths through the sample. In TOF-FRES, the flight time of the particles is determined in addition to their energy to distinguish the hydrogen isotopes from the large flux of elastically scattered He particles.[19] This procedure circumvents the need of a stopper foil conventionally used in a FRES experiment and improves the achievable depth resolution to some 23 nm at the film surface. As described previously,[7] the flight time information can in addition be used to gate the data acquisition system such that only the near-surface region is probed; we thereby avoid any overlap between the energy signals from hydrogen particles emerging from the film surface and deuterium particles emerging from deeper within the sample. This technique enables us to study films of arbitrary thickness and still unambiguously probe both hydrogen and deuterium in the near-surface region.[19]

Films of different bulk compositions have been investigated, which we shall refer to as blends III, IV, V, VI, and VII, relating to dPEP volume fractions of 0.31, 0.40, 0.50, 0.60, and 0.72, respectively. Only recently, Gehlsen and co-workers[17] have determined the temperature dependence of the effective Flory interaction parameter χ for the particular polymer mixture investigated in this study; from this we are able to construct the bulk phase diagram using the Flory–Huggins mean field approach. As can be seen in Figure 1, the bulk compositions chosen for the present study all fall well within the spinodal region of the phase diagram at 294 K; at 321 K we restrict ourselves to blends IV, V, and VI. It should be pointed out, however, that the mean field phase diagram shown in Figure 1 need not necessarily be correct; as a matter of fact, recent experiments do suggest deviations from mean field behavior. For the present, we shall take the mean field approximation as a rough guide; we shall return to the deviations from the mean field predictions at the end of the paper.

(b) Concentration versus Depth Profiles. In Figure 2 we show concentration versus depth profiles for a critical PEP/dPEP mixture (blend V) directly after film deposition and for a quench to 294 K. As reported earlier,[2,7] for critical compositions an oscillatory composition profile is

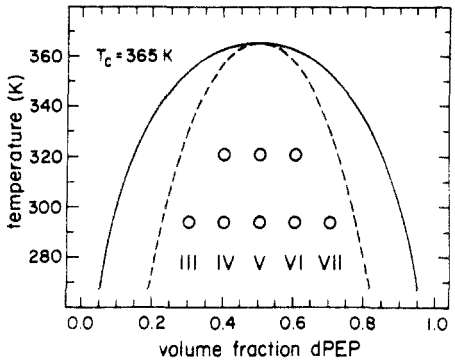

Figure 1. dPEP/hPEP phase diagram as calculated by Flory–Huggins mean field theory, using the value for $\chi(T)$ from ref 17. The different bulk compositions and quench locations are indicated.

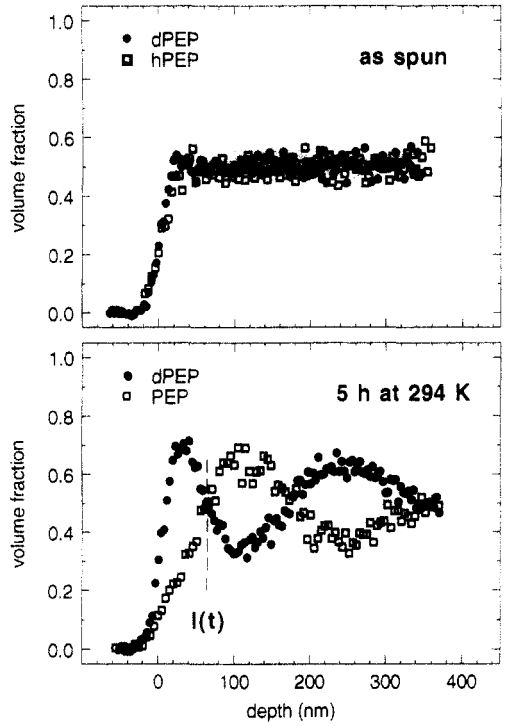

Figure 2. Volume fraction vs depth profiles for both dPEP (filled circles) and hPEP (open squares) as determined by TOF-FRES for the critical blend V: (a) as spun; (b) after annealing at 294 K for 5 h. The dashed line corresponds to the thickness $l(t)$ (see text). The data are cut at about 370 nm to avoid any overlap of the deuterium and hydrogen signals in the energy spectra.

observed with a dPEP layer wetting the film–vacuum interface followed by a PEP-rich layer in the subsurface region of the film. Due to the lower energy of the deuterated component, the phase separation leads to an almost prefectly ordered lamellar structure close to the surface which eventually decays into the isotropic domain structure as one moves from the surface toward the bulk of the sample. The same qualitative behavior is found for either quench depth.

In the case of off-critical bulk compositions, however, the situation is found to be more complex. For blends IV and VI, quenches to 294 K yield behavior which closely resembles that found for the critical mixture, with a second maximum in the dPEP composition profile clearly indicating the formation of at least one bilayer at the polymer–vacuum interface. As we get closer to the spinodal curve, however, the behavior changes and only a very shallow composition wave is observed. This can be seen in Figure 3, where we show composition vs depth profiles for blends III and VII after a quench to 294 K. The spectra no longer exhibit a well-defined second maximum in dPEP com-

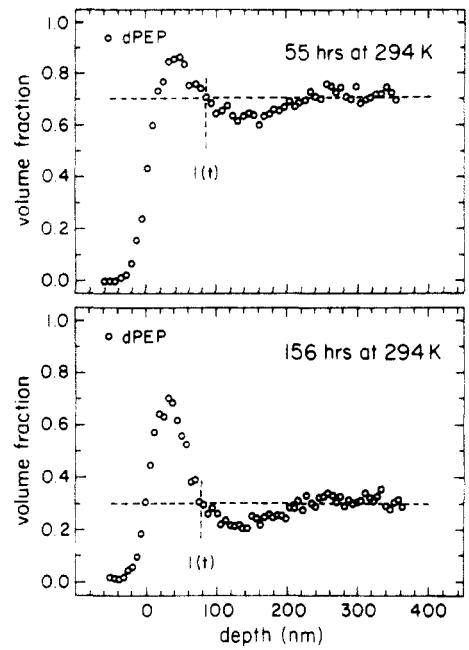

Figure 3. Volume fraction vs depth profiles for dPEP as determined by TOF-FRES for different off-critical quenches; (a) blend III, 294 K; (b) blend VII, 294 K. The horizontal dashed lines indicate the bulk dPEP volume fraction. The vertical lines correspond to the thickness $l(t)$ (see text). The data are cut at about 370 nm to avoid overlap of the deuterium and hydrogen signals in the energy spectra.

position, indicating that no lamellar structure is formed. In either of the cases shown in Figure 3, the composition vs depth profiles indicate the formation of a dPEP-rich surface layer, followed by a rather broad depletion zone over which the compositions gradually rise to their average bulk values.

(c) Wetting Layer Thickening. To study the time dependence of the composition waves, we may define a wetting layer thickness $l(t)$ as the depth where Φ_{dPEP} and Φ_{PEP} first match their bulk values. In the case of the critical mixture, $l(t)$ can be understood as the locus of the phase boundary between the two adjacent phases in the near-surface region. This interpretation may also hold for blends IV and VI after quenches to 294 K. For the situations shown in Figure 3, however, it should be pointed out that while $l(t)$ still may serve to quantify the surface layer thickness, it no longer has the meaning of a boundary separating adjacent domains as in the case of critical mixtures.

Figure 4 summarizes the results on the growth of $l(t)$ for the different quenches in a double-logarithmic presentation. For quenches to 294 K, we find that for all bulk compositions except blend VII the surface layer thickness $l(t)$ grows as $l(t) = a + bt^{1/3}$ (solid lines in Figure 4). From the values of a and b we may estimate a characteristic time $\tau = (a/b)^3$, after which $t^{1/3}$ growth should dominate. We find τ to be of order 4×10^4 s or $\ln(t) \approx 10.5$ (for blend V), in agreement with the observation that in the double-logarithmic presentation of Figure 4 a slope of $^1/_3$ (dashed line, right-hand side) is found only for times longer than a few tens of τ. It should be noted that this is only true for blends IV, V, and VI, whereas for blend III a slope of $^1/_3$ is not reached during the times accessible in the present experiment. The growth of the surface layer thickness for blend VII behaves quite differently. As can be seen in Figure 3 the data at sufficiently long times indicate a linear growth mode rather than the $t^{1/3}$ growth mode discussed above. Over the whole time range the growth of $l(t)$ is well represented by $l(t) = a + bt$ (dashed line).

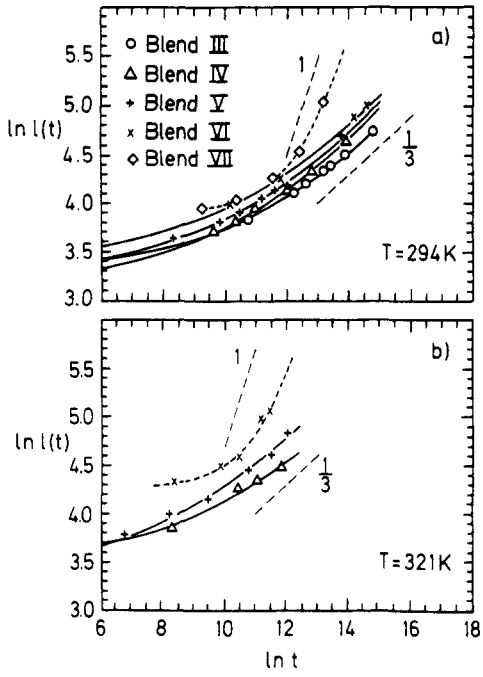

Figure 4. Thickness of the wetting layer as determined from the point where both Φ_{dPEP} and Φ_{PEP} are equal to the average composition for the first time (see Figures 2 and 3). The solid lines are least-squares fits to the data assuming $l(t) = a(T) + b(T)t^{\alpha}$ with $\alpha = 1/3$; the dashed lines assume $\alpha = 1$. The dashed lines next to the data points indicate slopes 1 and $1/3$, respectively. The average values of Φ_{dPEP} = 0.31 (○), 0.40 (△), 0.50, (+), 0.60 (×), 0.72 (diamonds).

For quenches to 321 K, the situation is similar in that the critical blend eventually shows $t^{1/3}$ growth at long times, whereas the thickness of the dPEP-poor blend (IV) is found to grow somewhat slower. Again, the dPEP-rich blend (VI) shows qualitatively different behavior—much faster surface layer growth.

(d) Dynamical Scaling of Profiles. Finally, we shall investigate whether the dynamical scaling behavior found for critical mixtures[7] is still observed for off-critical quenches. Given that $l(t)$ is the only relevant length scale in the near-surface region, we may construct rescaled profiles $n(z)$ as

$$n(z) = \Phi\left(\frac{z}{l(t)}\right) - \Phi_{avg} \qquad (1)$$

with Φ_{avg} being the bulk volume fraction of the respective species. The result of this procedure is shown in Figure 5 for blends III, V, and VII quenched at 294 K. We find that for all quenches studied in this paper the scaling prediction is indeed fulfilled in the near-surface region. Deviations do occur about one wavelength below the surface as expected; here $l(t)$ can no longer be regarded as the dominant length scale and the bulk domain size comes into play. The master curves, on the other hand, show qualitatively different features for different bulk volume fractions, reflecting the differences in the growth behavior discussed above.

III. Simulations

(a) Procedure. We have carried out three-dimensional cell-dynamical[20] simulations based on the Cahn–Hilliard–Cook equation[6,10,12] including surface interactions and nonlinearities. The starting point is the free energy

$$F = k_B T \int d^3r \{(\epsilon/2)\Psi^2 + (u/4)\Psi^4 + (c/2)\nabla^2\Psi + (\sigma_1\Psi + \sigma_2\Psi^2)\delta(z)\} \qquad (2)$$

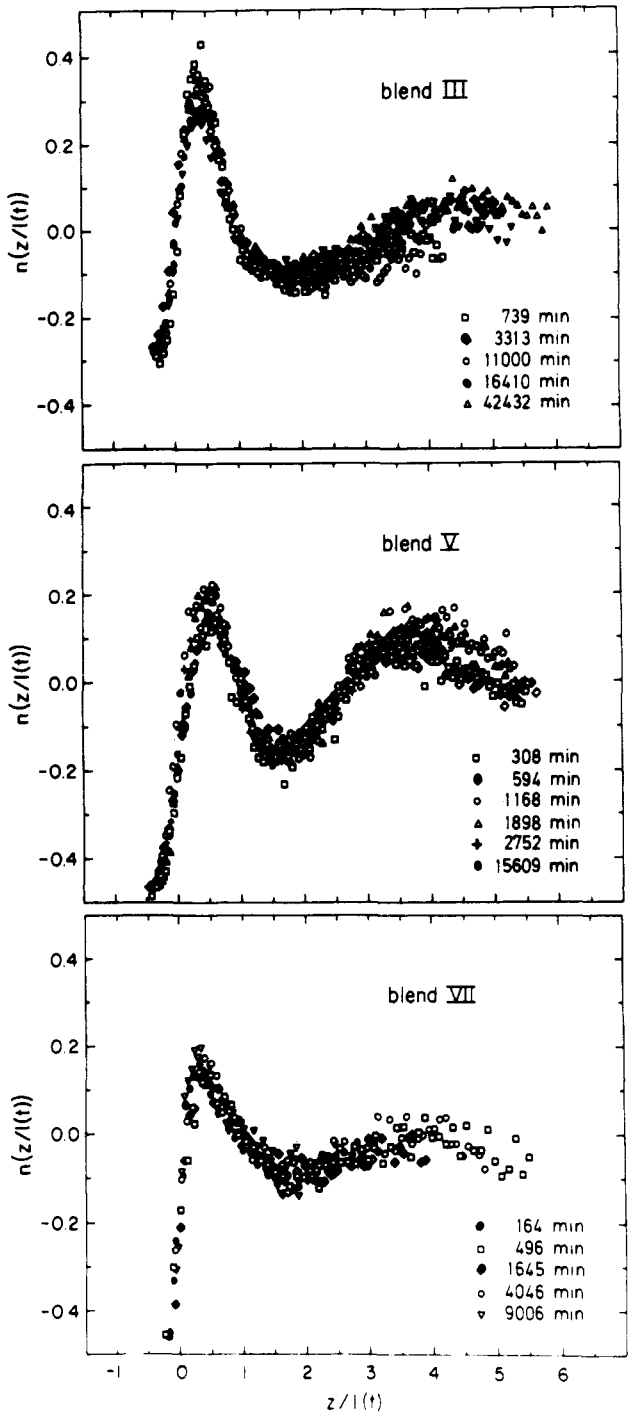

Figure 5. Deviation of the dPEP volume fraction from its average value, rescaled by the wetting layer thickness $l(t)$ according to eq 1 for quenches at 294 K.

where we have taken $\epsilon = 26.3(1 - T/T_c)/Nb^3$, $c = 0.83/b$, and $u = 5.0/Nb^3$, where b = 0.8 nm has been taken to be the monomer length (note that in our previous paper[6] we did not correctly report the numerical prefactors, which include a factor to correct for the number of actual monomers in a volume b^3).

The N and b scaling of these coefficients matches that of the Flory–Huggins–de Gennes[21] theory, and the prefactors have been chosen using (a) the behavior of the χ parameter previously reported for this system,[17] (b) quantitative knowledge of the thermal correlation length[22] ($\xi = (c/a)^{1/2}$ over a range of temperatures above T_c), and (c) the ratio $uNb^2/c = 6$ of the Flory–Huggins–de Gennes theory. The surface energies have been measured by Norton[23] for the dPEP–PEP system to be $k_B T\sigma_1 = 0.1$ mJ/cm^2 and $k_B T\sigma_2 = -0.01$ mJ/cm^2.

The CHC dynamics take the form of a conservation law relating order parameter current to gradients in chemical potential and a stochastic current:

$$\partial_t \Psi = \nabla\cdot\{M\nabla\delta F/\delta\Psi + \mathbf{j}(r,t)\} \quad (3)$$

where the effective diffusion constant is $D_{\text{eff}} = k_B T M\epsilon$ and where the noise $\mathbf{j}$ is a random vector with correlations

$$\langle j^\alpha(r,t)\, j^\beta(r',t')\rangle = 2Mk_B T\,\delta^{\alpha\beta}\,\delta(r-r')\,\delta(t-t') \quad (4)$$

We may rescale lengths by the thermal correlation length at the annealing temperature (T_f = 321 K), ξ = 20 nm. It is also useful to measure times in units of the diffusion time over that distance, which for an effective diffusion constant of $D_{\text{eff}} = 7 \times 10^{-15}$ cm^2/s (determined by a Cahn analysis of the early-time structure function evolution in the bulk[22]) is ξ^2/D_{eff} = 550 s. Finally, we rescale the field strength Ψ by its 321 K binodal values, which are $(u/\epsilon)^{1/2} = \pm 0.080$, corresponding to binodal volume fractions at 0.1 and 0.9.

The equation of motion for Ψ in rescaled units is[6,10,12]

$$\partial_t \Psi = \nabla^2\{\tau\Psi(r,t) + \Psi^3(r,t) - \nabla^2\Psi(r,t)\} + g^{1/2}\eta(r,t) \quad (5)$$

where $\tau = (T_i - T_c)/(T_c - T_f)$ for times $t < 0$ and $\tau = -1$ for times $t > 0$, T_c is the critical temperature, T_i is the temperature before the quench at time $t = 0$, and T_f is the temperature that the system is annealed at following the quench. We take T_c = 365 K, T_i = 409 K, and T_f = 321 K, which is a symmetric quench ($T_i - T_c = T_c - T_f$). The noise strength is $g = 2ua^{-1/2}c^{-3/2} \approx 2.5/[N(1 - T/T_c)]^{1/2}$. The correlation function for the noise is $\langle\eta(r,t)\,\eta(r',t')\rangle = -\nabla^2\delta(r-r')\,\delta(t-t')$. Finally, the effects of the surface are taken into account with a short-ranged interaction, which leads to a boundary condition at the surfaces

$$0 = \mathbf{n}\cdot\nabla\Psi + s_1 + s_2\mathbf{n}\cdot\Psi \quad (6)$$

where $s_1 = a^{-1}c^{-1/2}u^{1/2}\sigma_1$ and $s_2 = a^{-1/2}c^{-1/2}\sigma_2$;[6] at 321 K we thus have g = 0.15, s_1 = 0.59, and s_2 = −0.05. The unit vector $\mathbf{n}$ is the inward-pointing surface normal. With these choices of parameters, the $\Psi = +1$ ordered state is attracted by the substrate, which is supposed to be the polymer–vacuum interface; thus $\Psi = +1$ represents the dPEP-rich phase, and $\Psi = -1$ represents the PEP-rich phase.

The cell-dynamical simulations that we have used are a lattice realization of the rescaled model, with a lattice constant of about 1.25 times the unit of length (corresponding to about 24 nm) and a time step of about one-third of the unit of time (corresponding to about 70 s). The details of the dynamics and their connection to the CHC equation were discussed in a previous paper.[10] Our strategy here is to keep everything except the concentration the same as in our previous study[6] in order to understand just the effects of varying volume fraction.

In our previous study of thin layers of critical composition[6] we found that this model described the evolution of domain sizes after a quench to 321 K. Both the time and length scales are accounted for by this model, which has diffusion as the only transport mechanism. This, along with the observation that the surface layer thickness follows a $t^{1/3}$ growth law,[7] suggests that hydrodynamic flows are not playing a role in the critical-composition experiments at times up to 100 h after a quench. Our aim in this section is to present the simulation results for off-critical quenches without any hydrodynamic flows in order to study the effects of concentration where diffusion is the only transport mechanism operating.

All of our studies have been done with CDS simulations on a lattice with L = 64 elements in the x and y directions and H = 40 elements in the z direction. The thickness of our model samples is therefore 960 nm, about half the thickness of the layers studied in the experiments. We have chosen our system size to minimize computer time as much as possible, while keeping finite-size effects minimal.

Substrate boundary conditions as described above have been assumed on the surfaces z = 0 and z = 40. We note that we have assumed dPEP-attracting boundary conditions on both surfaces; in the experiments, the distant polymer–Si interface actually attracts the PEP component. We have checked that a change in the boundary condition at one wall does not substantially modify the behavior at the other for our choice of system size, and since we are concerned only with the experimental system behavior at the vacuum interface, we are able to double our statistical precision by analyzing the simulation behavior near both substrates.

For each concentration we ran four simulations, each with a different initial condition. The initial conditions (the state at t = 0) were determined by equilibration in the one-phase region for 1024 time steps at parameters corresponding to T = 409 K, starting with a uniform state $\Psi(r) = 2x_0 - 1$. We note that x_0 is the fraction that the net concentration is across the miscibility gap, with x_0 = 0 and 1 the binodal points. The equilibration period was sufficient for the volume fraction profile across the system to stabilize (a small enhancement of the order parameter near the substrates occurs about T_c). During each run, the configuration $\Psi(r,t)$ was periodically stored for later analysis.

We have studied the following concentrations: x_0 = 0.25, 0.40, 0.50, 0.60, and 0.75, which we will refer to as cases a–e, respectively, corresponding to net dPEP volume fractions of Φ_{avg} = 0.30, 0.42, 0.50, 0.58, and 0.70, respectively. The three concentrations near the critical concentration (b–d) all show spinodal decomposition in the bulk: the bulk is unstable after the quench into the two-phase region. However, the more asymmetric compositions (a and b) show nucleation behavior—the bulk is rather stable and remains mixed immediately after the quench.

In Figure 6 we show slices of $\psi(r,t)$ at fixed times for one of the runs at each concentration. For each case we show two slices of the system at each time, the y = 0 and y = 32 planes. The x axis runs horizontally (from x = 0 to x = 64 lattice positions, a total distance corresponding to about 1500 nm), and the z axis runs vertically (from z = 0 to z = 40, corresponding to 960 nm). The times run from top to bottom in each case and are (in CDS time steps) t = 304, 512, 1024, 2048, 4096, and 8192. These correspond to experimental annealing times of about 5.8, 10, 20, 40, 80, and 160 h. The black regions adjacent to the substrates have $\Psi > 0$ and reprsent dPEP-rich regions; the white regions have $\Psi < 0$ and represent PEP-rich regions.

Figure 6 shows evidence of asymmetry in the shape of the domains as x_0 is moved away from the critical concentration 0.5. For x_0 = 0.25, case, we see only a wetting layer, which thickens with time. Contrast this with x_0 = 0.75, case e, where there is a wetting layer of the dark phase, but in this case, isolated minority phase droplets appear near the substrates at a time of about 512 steps after the quench. At near-critical concentrations (cases b–d), we see interconnected patterns characteristic of spinodal decomposition: these appear immediately after the quench. In each case, by 304 time steps, the domain interiors are nearly saturated. We note that in cases a and e, bulk spinodal decomposition does not occur, indicating that for these concentrations bulk domain

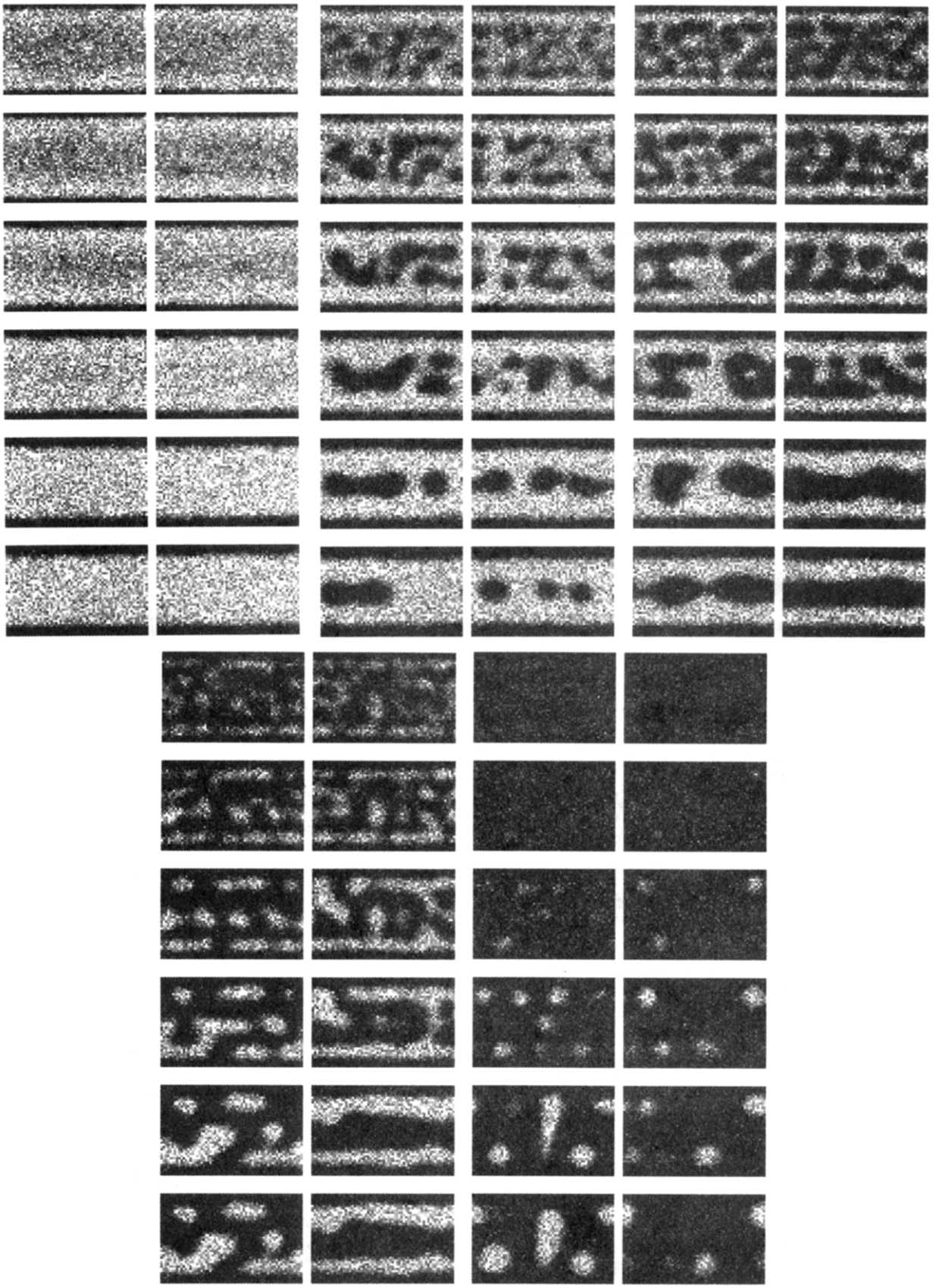

Figure 6. Slices of $\psi(r,t)$ at fixed times: parts a–e show rescaled net concentrations $x_0 = 0.25$, 0.40, 0.50, 0.60, and 0.75, respectively (x_0 is the fraction that the bulk concentration is across the mean field miscibility gap). For each case we show two slices of the system at each time, the $y = 0$ and $y = 32$ planes. The x axis runs horizontally (from $x = 0$ to $x = 64$ lattice positions, a total distance corresponding to about 1500 nm), and the z axis runs vertically (from $z = 0$ to $z = 40$, corresponding to 960 nm). The times run from top to bottom in each case and are (in CDS time steps) $t = 304$, 512, 1024, 2048, 4096, and 8192. These correspond to experimental annealing times of about 5.8, 9.8, 20, 40, 80, and 160 h. The black regions adjacent to the substrates have $\Psi < 0$ and represent PEP-rich regions; the white regions have $\Psi < 0$ and represent PEP-rixh regions.

growth will proceed only after a time sufficient to allow activation of stable minority phase nuclei.

We note that we have estimated parameters for this model for the quench to 321 K but that many of the

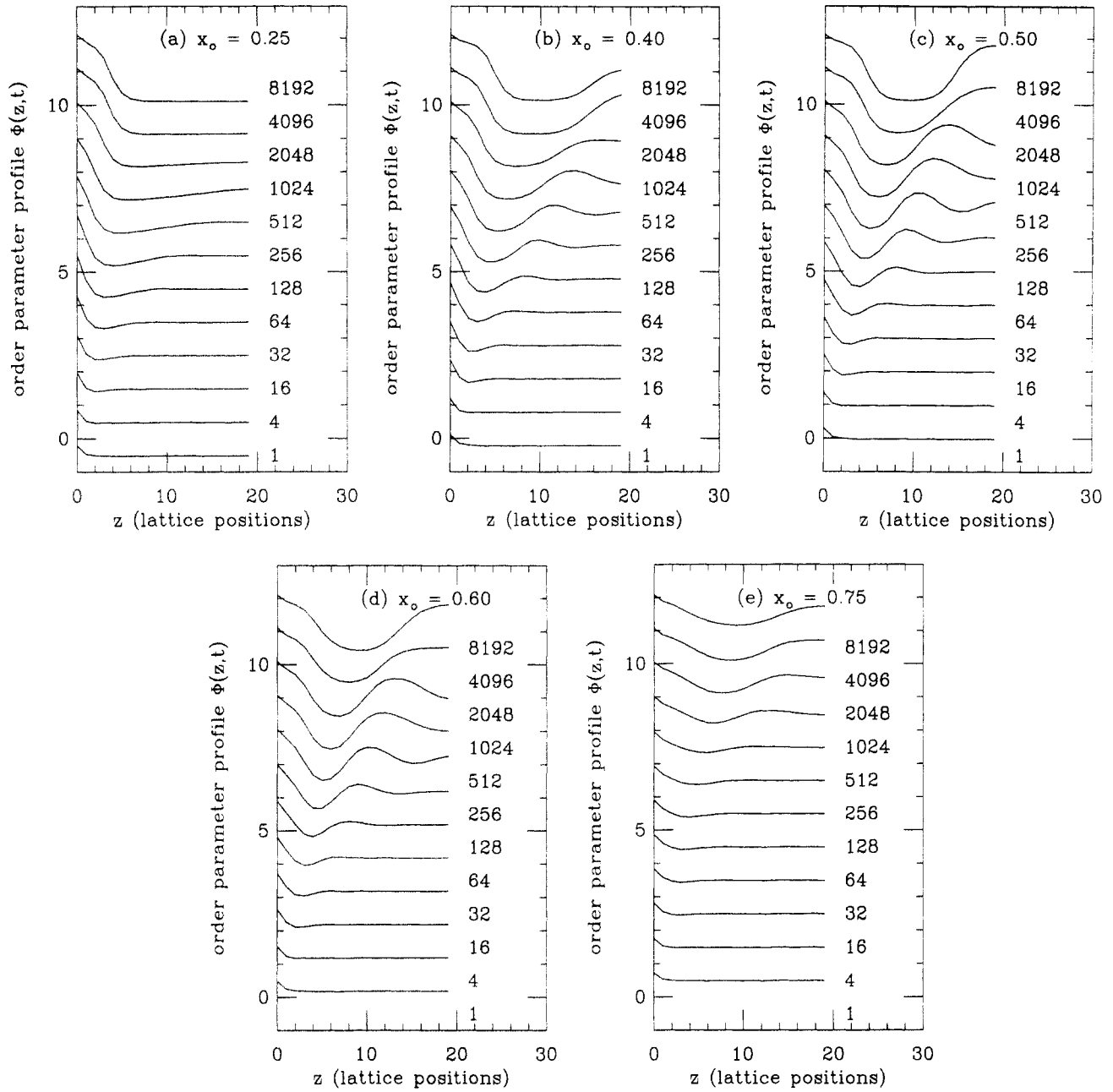

Figure 7. Simulation vertical order parameter profiles $\Phi(z,t)$ for a series of times from 1 to 8192 time steps: successively later times are offset by 1. Parts a–e show rescaled concentrations x_0 = 0.25, 0.40, 0.50, 0.60, and 0.75, respectively.

comparisons will be with the experimental data for quenches to 294 K. The trends with concentration that we will discuss are the same for either experimental quench.

(b) Volume Fraction vs Depth Profiles. Our simulation data were analyzed to yield volume fraction profiles $\Phi(z,t) = \int dx\, dy\, \Psi(r,t)/L^2$; the eight profiles for each bulk concentration were then averaged to give the results reported here. In Figure 7a–e we show the simulation profiles for a series of times from 1 to 8192 time steps ($\Phi(z,t)$ at successively later times are offset by 1).

In each case, we observe formation of a wetting layer at $z = 0$ (and a value of $\Phi(z=0,t) \approx +1$) and above it, a depletion zone (where $\Phi(z,t) \leq 2x_0 - 1$) corresponding to an excess of the nonwetting component. The shapes of the profiles in the three cases that show spinodal decomposition (b–d) are rather similar—in each case an oscillating profile appears. However, in cases a and e, we see that the depletion zone is shallow compared to the bulk value $2x_0 - 1$, in comparison with the quenches near the critical concentration. This is true in the experiments as well (see Figure 5).

Interestingly, in case a, the lack of formation of any dark domains between the wetting layers allows the phase separation to quickly become nearly complete, as evidenced by the drop of $\Phi(z=20,t)$ in that case for times beyond about 512. This corresponds roughly to the simple diffusion time (of order $(H/2)^2 = 400$ time steps) halfway across the z extent of the system. After this time, there are strong finite size effects in this case since the depletion zone effectively extends across the entire system.

(c) Wetting Layer Thickening. The wetting layer thickness $l(t)$ is defined as in the experiment, by finding the smallest $l(t)$ that solves

$$\Phi(z=l(t),t) = 2x_0 - 1 \tag{7}$$

This procedure leads to the layer thicknesses shown in Figure 8, plotted on a double-logarithmic graph (thickness is in units of lattice constants, time is in units of time steps, natural logarithms are used). The straight line has slope $^1/_3$. In each case, the layer thickness grows at a rate comparable to the $t^{1/3}$ bulk domain growth law expected for the CHC model. There is a rapid increase in $l(t)$ in

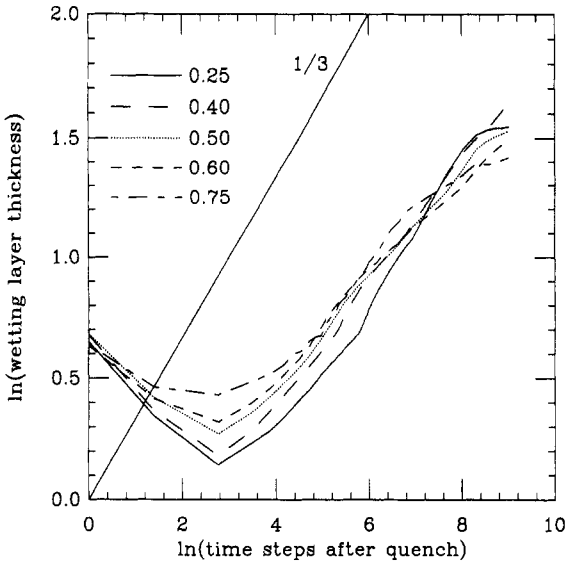

Figure 8. Surface layer thickness plotted on a double-logarithmic graph (thickness is in units of lattice constants, time is in units of time steps, natural logarithms are used). The straight line has slope $^1/_3$. The rate of growth of the wetting layer is always comparable with the diffusive ($t^{1/3}$) growth law.

case a after ln(t) = 6 (for $t > 400$ time steps corresponding to about 7.7 h) due to the extension of the depletion zone across the system. However, the rates of growth in case a stay comparable to those observed for other concentrations throughout the entire phase separation process. At early times (ln $t < 6$), there is a slight retardation of the layer thickening as x_0 is decreased below 0.5 and a slight acceleration as x_0 is increased above 0.5, in agreement with the experimental trend (see Figure 4).

The main result of the simulations is that over a wide range of concentrations, the diffusive CHC dynamics lead to surface layer thickening at a rate comparable to the $t^{1/3}$ growth law observed in the bulk. The same conclusion was reached from separate CHC studies in two dimensions at various concentrations, where one can more easily study the large-system-size limit.[8,24] We conclude that the experimental mixtures III–VI at 294 k and IV–V at 321 K are described by the CHC diffusive coarsening model. However, diffusive dynamics cannot explain the rapid increase of $l(t)$ observed in experimental case VII (Φ_{avg} = 0.72) at 294 K and case VI (Φ_{avg} = 0.60) at 321 K.

IV. Discussion

(a) Diffusive Surface Layer Growth. A $t^{1/3}$ growth law was predicted for the growth via diffusion of bulk domains during spinodal decomposition for times when the domain compositions have already reached their equilibrium value and only the size of the domains is growing with time.[14,25] An argument similar to that applied to bulk coarsening can be used to predict the late-stage growth of the surface layer:[10] assume a wetting layer of thickness l to be in contact with bulk domains of size R. The scale for the chemical potential in the surface layer μ_{surf} ($=\mu_{surf,PEP} - \mu_{surf,dPEP}$) may be estimated to vary with l as $\mu_{surf} \approx \sigma/l$, with σ being the interfacial energy of the phase boundary. Variations of μ_{surf} are then expected to occur over distances l;[26] i.e., $\nabla\mu_{surf} \approx \sigma/l^2$. By Fick's law, this weak gradient is μ_{surf} will drive a flux which in turn leads to a thickening of the surface layer, and we therefore find $dl/dt \approx \sigma/l^2$ or $l(t) \approx t^{1/3}$. For the case of critical mixtures, $t^{1/3}$ surface layer growth was observed in computer simulations.[8,10]

As we have discussed, our simulation results can be mapped onto the experimental system studied here by identifying one time step with 70 s (for T = 321 K). From Figure 8 (see also Figure 6 of ref 10) we estimate a characteristic time of about 150 steps (ln(150) ≈ 5) or 8.1 × 10^4 s for the onset of $t^{1/3}$ growth. This value is close to the experimental value $\tau = 4 \times 10^4$ s estimated from Figure 4.

The scaling argument given above is not restricted to critical mixtures, but it does assume that there be no means of transporting material other than diffusion. The preliminary simulation results discussed here indicate that the surface layer thickens at $t^{1/3}$ for off-critical quenches, even where there is a nucleation barrier to be crossed before coarsening can occur. As we have discussed above, the experiments at 294 K with dPEP fractions less than 0.69 and those at 321 K with dPEP fractions less than 0.60 all show surface layer thickening that is consistent with the simulations, indicating that diffusion is the predominant transport process causing domain growth in those cases.

In the experiments on the dPEP-poor blends III (294 K) and IV (321 K), the growth of the wetting layer is found to be slowed down and the $t^{1/3}$ regime is not quite reached within the times accessible in the present experiment. In our simulations where the minority phase is wetting the substrate, we have observed such a retardation of the surface layer growth before finite-size effects set in (Figure 8).

An explanation of this effect is that the enrichment of the surface layer drives the adjacent subsurface region toward the metastable nucleation regime of the phase diagram even for a quench inside the bulk spinodal. This change would cause the growth of the wetting layer to be retarded since transport of the minority component must occur across a relatively stable majority phase layer. An additional factor is that recent experimental evidence[27] indicates that the PEP/dPEP bulk phase diagram deviates considerably from the mean field prediction, with equilibrium binodal compositions falling well inside the coexistence curve shown in Figure 1. Thus the far-off-critical quenches may be nearer (or even inside) the nucleation region than one would expect from the mean field phase diagram.

It should be pointed out that this $t^{1/3}$ growth behavior found during phase ordering is qualitatively different from what has been found for wetting phenomena in the one-phase region. Steiner and co-workers only recently reported complete wetting from a binary polymer mixture of binodal composition.[28] In this situation, where the wetting layer is in contact with an "infinite" reservoir of material, a logarithmic growth law is observed.

(b) Lowering of Nucleation Barriers near a Surface. We have observed a novel phenomenon in our simulations of off-critical quenches when the majority phase is attracted by the substrate and when there is nucleation and growth in the bulk due to metastability of the initial, mixed state. This situation is encountered in case e of our simulations. The majority phase is expelled from the immediate vicinity of the substrate and thus becomes more highly concentrated than in the bulk over a thermal correlation length or so above the substrate. The nucleation barrier in that region can be reduced or eliminated near the substrate, leading to much earlier formation of domains of minority phase near the surface than in the bulk. We have observed this effect in separate simulation studies in two dimensions, and we plan to report on it in more detail elsewhere.[24]

(c) Fast Surface Layer Growth. Consider the results for the quenches of the most dPEP-rich blends: at 321 K, case VI, and at 294 K, case VII. For these dPEP-rich cases, the wetting layer thickness is found to grow considerably faster than the $t^{1/3}$ behavior discussed above,

an effect not observed in the simulations. Considering the concentration vs depth profiles (Figure 3), the simulations (Figure 6e), and the arguments of the previous subsection, we are led to visualize a dPEP-rich surface layer and small isolated droplets of the hPEP minority phase "lining up" adjacent to it. The number density of these droplets is somewhat larger than in the bulk, yet no continuous hPEP-rich layer can be formed (as can be seen from the fact that the maximum value of Φ_{hPEP} does not reach the respective value found for critical quenches (Figure 2)). Thus, d-PEP-rich material can easily undergo hydrodynamic flow through the connected dPEP-rich phase, passing around the hPEP-rich domains. This situation is distinctly different from the growth of $l(t)$ when there is a lamellar domain structure near the substrate.

If this picture is correct, we expect surface layer thickening similar to that observed for domain growth in the bulk via hydrodynamic flow driven by interfacial tension,[10,13] i.e., $l(t) \approx (\sigma/\eta)t$, where η is the fluid viscosity. As can be seen in Figure 4, the data are described by a linear growth law at the latest times. The experimental linear growth rate is $d\,l(t)/dt \approx 2.5 \times 10^{-10}$ cm/s (321 K). For hydrodynamic growth we expect $d\,l(t)/dt \approx \sigma/\eta$, where σ is the interfacial tension and η is the viscosity. With $\sigma \approx 1.7 \times 10^{-3}$ dyn/cm[29] and $\eta \approx 1.3 \times 10^{6}$ P,[30] respectively, we find $d\,l(t)/dt \approx 1.3 \times 10^{-9}$ cm/s. This rather rough estimate lends further support to this suggestion that hydrodynamic effects may come into play in the surface layer thickening for quenches with a high dPEP volume fraction.

V. Conclusions

We have experimentally investigated the effects of a surface on the spinodal decomposition in a binary polymer mixture for quenches to different locations in the phase diagram. It was found that distinct differences occur in the vicinity of the surface depending on whether the wetting phase is the minority or the majority component in the mixture. While the minority phase tends to build up to a surface layer somewhat slower than for critical mixtures, the majority phase was found to wet the surface in a distinctly faster process, possibly due to hydrodynamic flows. Independent of the initial bulk composition, however, all mixtures studied exhibit dynamic scaling behavior.

We have also studied computer simulations of the Cahn–Hilliard–Cook equation near a substrate that wets one of the phases. This model for phase ordering contains no hydrodynamic flows, and the only transport process is diffusion. We see no strong acceleration of the surface layer thickening when the majority phase is attracted by the substrate: the rates for thickening of the surface layer are well described by the "diffusive" $t^{1/3}$ law. Finally, our simulations strongly suggests that the expulsion of a nonwetting minority phase from the vicinity of a substrate may cause reduction of local nucleation barriers at early times. This can lead to preferential formation of minority phase domains near the substrate.

Acknowledgment. This work was supported by the NSF–DMR Polymers Program (Grant No. DMR-9223099). G.K. greatly appreciates financial support through the Max Kade Foundation, New York, F.S.B. is indebted to the NSF for support through Grant No. DMR-8957386. J.F.M. was supported by the MRL program of the NSF under Award No. DMR-9121654 and he thanks M. Geoghegan for communicating the results of his experiments. Acknowledgment is made to the donors of the Petroleum Research Fund, administered by the American Chemical Society, for partial support of this work at Kansas State University and to the Pittsburgh Supercomputing Center for a grant of supercomputer time. G.B. is a recipient of a National Science Foundation predoctoral fellowship. We thank L. J. Norton, M. H. Rafailovich, and J. Sokolov for helpful discussions. The skillful help of N. Szabo and P. Revesz during the course of the experiments is gratefully acknowledged.

References and Notes

(1) Ball, R. C.; Essery, R. L. H. *J. Phys. Condens. Matter* **1990**, *2*, 10303.
(2) Jones, R. A. L.; Norton, L. J.; Kramer, E. J.; Bates, F. S.; Wiltzius, P. *Phys. Rev. Lett.* **1991**, *66*, 1326.
(3) Bruder, F.; Brenn, R. *Phys. Rev. Lett.* **1992**, *69*, 624.
(4) Cumming, A.; Wiltzius, P.; Bates, F. S.; Rosedale, J. H. *Phys. Rev. A* **1992**, *45*, 885. Wiltzius, P.; Cumming, A. *Phys. Rev. Lett.* **1991**, *66*, 3000.
(5) Tanaka, H. *Phys. Rev. Lett.* **1993**, *70*, 53, 2770.
(6) Krausch, G.; Dai, C.-A.; Kramer, E. J.; Marko, J. F.; Bates, F. S. *Macromolecules* **1993**, *26*, 5566.
(7) Krausch, G.; Dai, C.-A.; Kramer, E. J.; Bates, F. S. *Phys. Rev. Lett.* **1993**, *71*, 3669.
(8) For critical-composition CHC dynamics in two dimensions, see: Brown, G.; Chakrabarti, A. *Phys. Rev. A* **1992**, *46*, 4829. For a minority wetting phase in two dimensions, see: Toral, R.; Chakrabarti, A. *Phys. Rev. B* **1991**, *43*, 3438.
(9) Puri, S.; Binder, K. *Phys. Rev. A* **1992**, *46*, R4487.
(10) Marko, J. F. *Phys.Rev. E* **1993**, *48*, 2861.
(11) Troian, S. *Phys. Rev. Lett.* **1993**, *71*, 1399.
(12) Gunton, J. D.; San Miguel, M.; Sahni, P. S. In *Phase Transitions and Critical Phenomena*; Domb, C., Lebowitz, J., Eds.; Academic Press: London, 1983; Vol. 8.
(13) Siggia, E. D. *Phys. Rev. A* **1979**, *20*, 595.
(14) Lifshitz, I. M.; Slyozov, V. V. *J. Phys. Chem. Solids* **1961**, *19*, 35.
(15) Bates, F. S.; Rosedale, J. H.; Bair, H. E.; Russell, T. P. *Macromolecules* **1988**, *21*, 1086.
(16) Bates, F. S.; Wignall, G. D.; Koehler, W. C. *Phys. Rev. Lett.* **1985**, *55*, 2425.
(17) Gehlsen, M. D.; Rosedale, J. H.; Bates, F. S.; Wignall, G. D.; Hansen, L.; Almdal, J. *Phys. Rev. Lett.* **1992**, *68*, 2452.
(18) Jones, R. A. L.; Kramer, E. J.; Rafailovich, M. H.; Sokolov, J.; Schwarz, S. A. *Phys. Rev. Lett.* **1989**, *62*, 280.
(19) Sokolov, J.; Rafailovich, M. H.; Jones, R. A. L.; Kramer, E. J. *Appl. Phys. Lett.* **1989**, *54*, 590.
(20) Oono, Y.; Puri, S. *Phys. Rev. Lett.* **1987**, *58*, 836. Oono, Y.; Puri, S. *Phys. Rev. A* **1988**, *38*, 434. Oono, Y.; Puri, S. *Phys. Rev. A* **1988**, *38*, 1542. Shinozaki, A.; Oono, Y. *Phys. Rev. Lett.* **1991**, *66*, 173.
(21) de Gennes, P.-G. *Scaling Concepts in Polymer Physics*; Cornell University Press: Ithaca, NY, 1985.
(22) Kredowski, C.; Bates, F.; Wiltzius, P. *Macromolecules* **1993**, *26*, 3448.
(23) Norton, L. Ph.D. Thesis, Cornell University, 1994.
(24) Brown, G.; Chakrabarti, A.; Marko, J. F., Preprint, 1993.
(25) Huse, D. A. *Phys. Rev. B* **1986**, *34*, 7845.
(26) We might as well assume that μ_{surf} varies over distances R rather than l. Since $R(t) \approx t^{1/3}$, however, this leads to $l(t)^2 \approx t^{2/3}$ or again $l(t) \approx t^{1/3}$.
(27) Heier, J.; Krausch, G.; Kramer, E. J.; Bates, F. S., to be published.
(28) Steiner, U.; Klein, J.; Eiser, E.; Budkovski, A.; Lewis, L. J. *Science* **1992**, *258*, 1126.
(29) We estimate $\sigma \approx k_B T/\xi^2$ with $k_B T = 4 \times 10^{14}$ erg and the bulk correlation length $\xi = 49$ nm.
(30) We estimate η from the rheological data reported in ref 22.